Histol Histopathol (2020) 35: 97-109

http://www.hh.um.es

Histology and Histopathology
From Cell Biology to Tissue Engineering

Hypertension accelerates age-related intrarenal small artery (IRSA) remodelling and stiffness in rats with possible involvement of AGEs and RAGE

Yajing Bai[1], Xiaoyun Shi[2], Yilang Ke[2], Xiaohong Lin[3] and Huashan Hong[2]

[1]Department of Intensive Care Unit, [2]Department of Geriatrics and

[3]Department of Emergency, Fujian Medical University Union Hospital, Fuzhou, Fujian, China

Summary. Objectives. To study changes in morphology, advanced glycation end products (AGEs) and the AGEs receptor, RAGE, that occur with ageing in intrarenal small arteries (IRSAs) of spontaneously hypertensive rats (SHRs) and to investigate the possible roles of hypertension, AGEs and RAGE in the progression of IRSA remodelling and stiffness with ageing in rats. METHODS: Ageing SHRs and ageing normotensive Wistar Kyoto (WKY) rats were studied. The minimal renal vascular resistance (minRVR) was measured. Renal arcuate arteries (RAAs) and interlobular arteries (RILAs), the expression of α-smooth muscle actin, proliferating cell nuclear antigen, AGEs, RAGE and the plasma concentrations of AGEs were also examined. RESULTS: The IRSA minRVR, wall thickening, cell proliferation and collagen deposition in RILAs and RAAs gradually increased with age in SHRs and were much higher in 24-week-old SHRs than in age-matched WKY rats ($p<0.05$); these indexes in WKY rats were only elevated in the 72-week group ($p<0.05$). The expression of RAGE in the RAA and RILA tunica media in SHRs was upregulated by 24 weeks and 12 weeks ($p<0.05$), respectively, while AGEs levels in the plasma and in the IRSA tunica media were increased by 48 weeks ($p<0.05$) and increased gradually with age. The levels of both RAGE and AGEs in WKY rats were increased only at 72 weeks ($p<0.05$). CONCLUSION: Hypertension accelerates the development of age-related IRSA remodelling and stiffness in rats, which may be related to upregulation of RAGE in the IRSA tunica media and increased expression of AGEs at the late stage.

Key words: Hypertension, Ageing, Intrarenal small artery, Advanced glycation end products, RAGE

Offprint requests to: Huashan Hong, MD, Department of Geriatrics, Fujian Medical University Union Hospital, Fujian Key Laboratory of Vascular Aging (Fujian Medical University), 29 Xinquan Road, Fuzhou 350001, Fujian, China. e-mail: 15959159898@163.com

DOI: 10.14670/HH-18-141

Introduction

Generalized arterial stiffness is a sign of natural ageing and is characterized by reduced vascular compliance due to age-related decreases in the ability to cope with physiological stress. Arterial stiffness is a common process of progressive irreversible ageing

Abbreviations. AGEs, advanced glycation end-products; α-SMA, α-smooth muscle actin; BAG3, Bcl-2-associated athanogene 3; CSA, medial cross-sectional area; CSAtot, total cross-sectional area; CSA%, CSA/CSAtot; ELISA, enzyme linked immunosorbent assay; EVG, Elastica van Gieson stain; HE, hematoxylin and eosin; IPP, Image-Pro Plus; IRSA, intrarenal small artery (arterial); MAPK, mitogen activated protein kinase; minRVR, minimal renal vascular resistance; MT/ED, medial thickness/external diameter; MT/IDshort, medial thickness/short internal diameter; NF-κB, nuclear factor-kappaB; OD, average optical density; PBS, phosphate buffered solution; PCNA, proliferation cell nuclear antigen; PI, proliferation index; RAA, renal arcuate arteries (arterial); RAGE, receptor for AGEs; RILA, renal interlobular arteries (arterial); ROS, reactive oxygen species; SBP, systolic blood pressure; SHR, spontaneously hypertensive rat; VSMC, vascular smooth muscle cell; WKY, wistar-kyoto.

leading to target organ damage (Janić et al., 2014; Sehgel et al., 2015a,b). It has been found from autopsies that ageing can cause decreased compliance in intrarenal small arteries (IRSAs), resulting in renal ischaemia and the occurrence and development of cardiovascular disease (Vavrinec et al., 2012; Denic et al., 2016). A recent study has shown that age-related vascular remodelling in people with essential hypertension progresses faster than that in normal individuals (Bruno et al., 2017). The vicious cycle between hypertension and the IRSA remodelling caused by hypertension is well known; however, whether hypertension accelerates age-related IRSA remodelling and stiffness and its mechanisms are still not understood.

Advanced glycation end products (AGEs) are a group of structurally highly heterogeneous irreversible active products that are formed by non-enzymatic glycosylation (the Maillard reaction) between the carbonyl groups of reducing sugars and lysine ε-amino groups on proteins, lipids and nucleic acids present in plasma or tissues (Singh et al., 2001). AGEs can cause the occurrence of arterial remodelling and stiffness by promoting the proliferation and phenotype transition of vascular smooth muscle cells (VSMCs) (Ma et al., 2015; Li et al., 2017), causing changes in elastic components and their arrangement (McRobert et al., 2012) and promoting the secretion of collagen (Li et al., 2012) through direct regulation of protein cross-linking or by binding to their specific receptor, RAGE (Sun et al., 2016). As a multi-ligand receptor, RAGE can also be involved in the process of arterial stiffening through mechanical stretch signalling, endocrine factor stimulation, or interaction with other ligands, such as S100/calcineurin and amphiregulin/high speed haematocrit box protein (HMGB1) (Li et al., 2012; Liu et al., 2013; Chaabane et al., 2015).

Studies on the roles of AGEs and RAGE in arterial remodelling and stiffness have thus far focused on large arteries, such as the aorta (Wu et al., 2013). However, a clinical cross-sectional study in 2013 (n=1192) studied the correlation between plasma AGEs and pulse wave velocity (PWV), central enhancement index (cAI) and peripheral enhancement index (pAI) with regards to multiple influencing factors and revealed that there was a greater correlation between peripheral arterial stiffness and plasma AGEs than between aortal stiffness and AGEs (Huang et al., 2013). As IRSAs are small muscular arteries that govern blood redistribution in the kidney, IRSA stiffness plays an important role in ageing-induced renal insufficiency (Franchi et al., 2016). However, there has been little research on age-related IRSA remodelling and stiffness under normal blood pressure and hypertension; moreover, there has been no report on the relationship between AGEs, RAGE and IRSA remodelling and stiffness.

Based on the above information, we investigated the dynamic changes in the minimal renal vascular resistance (minRVR) and morphology of IRSAs, the expression of vascular AGEs and RAGE and the plasma levels of AGEs in SHRs and WKY rats during ageing. The aim of the study was to elucidate the following: (1) whether hypertension can accelerate and aggravate age-related IRSA remodelling and stiffness and (2) whether AGEs and RAGE are involved in hypertension-related induction of the development and progression of IRSA remodelling and stiffness.

Materials and methods

Animals

Specific pathogen-free (SPF) male SHRs and WKY rats at 3 weeks old were purchased from the Shanghai SLAC Laboratory Animal Company (License No: SCXK (Shanghai) 2012-0002). The rats were raised in separate cages in the SPF facility in the Laboratory Animal Center of Fujian Medical University (permit number SYXK (Fujian, China) 2008-0001). The photoperiod was manually controlled (light 12 h, dark 12 h). The temperature was maintained at 22-24°C, and the relative humidity was 45-55%. The rats were fed a standard diet with no food or water restrictions. All animal studies were conducted in compliance with the national laboratory animal regulations and the Fujian Regulations of Laboratory Animal Management and were approved by the Institutional Animal Care and Use Committee of Fujian Medical University (Fuzhou, Fujian, China).

Methods

Experimental groups

After one week of adaptive feeding, the SHRs were randomly divided into 5 experimental groups (n=16 for each group): a 4-week group, a 12-week group, a 24-week group, a 48-week group and a 72-week group. Age-matched WKY rat groups were used as control groups.

Measurement of body weight and blood pressure

The animals were measured for body weight (g) and blood pressure, including systolic blood pressure, diastolic blood pressure and mean arterial pressure (mmHg) using a non-invasive blood pressure meter (SoftronBP-2010 Series, Beijing Incorporated, China) according to the Shi et al. (2018) method.

Minimal renal vascular resistance (Song et al., 2011)

Eight SHRs and 8 WKY rats at 4 (SHR/WKY 4-week groups), 12 (SHR/WKY 12-week groups), 24 (SHR/WKY 24-week groups), 48 (SHR/WKY 48-week groups) and 72 (SHR/WKY 72-week groups) weeks of age (a total of 40 SHRs and 40 WKY rats) were anaesthetized with intraperitoneal pentobarbital sodium (60 mg/kg). As shown in Fig. 1, A tracheotomy was

performed, and a midline abdominal incision was made. The abdominal aorta was isolated 1 cm proximally and distally to the opening of left renal artery. The right renal artery and left adrenal gland artery were ligated. The mesenteric artery was cannulated to allow measurement of aortic pressure close to the left renal artery (i.e., renal arterial inflow pressure). Following heparinization (3000 U/kg, intravenous), a catheter connected to the perfusion setup was inserted retrogradely through the abdominal aorta to a position distal to the left renal artery. The aorta was ligated just above the mesenteric artery to make a closed arterial circuit including the left kidney, and the left renal vein was cut.

Then, perfusion of the left kidney was begun with 37°C oxygenated (95% O_2 and 5% CO_2) artificial Krebs saline (118.3 NaCl, 4.7 KCl, 1.2 $MgSO_4$, 1.2 KH_2PO_4, 24.2 $NaHCO_3$, 11.0 GLU, 2.52 $CaCl_2$, 0.00047 g/L EDTA, pH=7.40) with a peristaltic pump (ALC-RP Shanghai Alcbio. Ltd., China). The flow rate was initially maintained at 3.0 ml/min (except for the 4-week group, for which it was maintained at 1.0 ml/min). Thirty minutes after the initiation of renal perfusion, measurements of arterial inflow pressure were repeated during seven or eight stepwise increases in perfusion flow from 3 to 15 ml/min (except for the rats in the 4-week group, for which flow was increased from 1.5-7 ml/min). After taking final measurements, the weight of the left kidney was measured.

In maximally vasodilated perfused kidneys, neurohumoral and active autoregulatory control systems are assumed to be inoperative; therefore, analysis of haemodynamic behaviour enabled us to perform functional assessments of structural properties in the renal resistance vessels (Huang et al., 2013). In the flow (inflow rate)-pressure relationship, the slope of the trend line is the minimal renal vascular resistance (minRVR) at maximal dilatation. The inflow rate (ml/min per gram) =perfusion flow/left kidney wet weight.

Intrarenal small artery specimen preparation

The rest of the rats in each group were anaesthetized, and the abdominal aorta was isolated as described above. The right renal artery, left adrenal gland artery and abdominal aorta just under the mesenteric artery were ligated. A catheter connected to the perfusion setup was inserted retrogradely through the abdominal aorta to a position distal to the left renal artery, and the left renal vein was cut. Perfusion of the left kidney was initiated with 4°C oxygenated Krebs saline, and the flow rate was maintained at 2.0 ml/min (except for the 4-week-group, for which it was maintained at 0.2 ml/min) until the colour of the left kidney became ash grey. Then, continuous perfusion with 4% paraformaldehyde (pH=7.2-7.4) was performed for 30 minutes. The left kidney was taken and washed in cold saline solution; then, the attached tissues were removed, and the kidney was cut in half along the coronal plane. The ventral renal part was fixed in 4% paraformaldehyde, embedded in paraffin, sectioned consecutively with a Leica microtome (RM2245 Leica, Germany) into 4 μm-thick left kidney slices. The slices were sequentially stained with HE, Elastic van Gieson (EVG), and picric acid-Sirius red, and immunofluorescence staining was performed with an α-SMA antibody. In addition, the slices were stained immunohistochemically with AGE, RAGE and PCNA antibodies.

Morphometric analysis of renal arcuate and interlobular arteries (Skov et al., 1992; Reddi et al., 2001; Chilton et al., 2011)

The left kidney slices (4 μm thick) were stained with Elastic van Gieson (EVG, Beijing Zhongshan Golden Bridge Biotechnology Inc., Beijing, China) to assess elastic fibres (purple-coloured) and examined with a

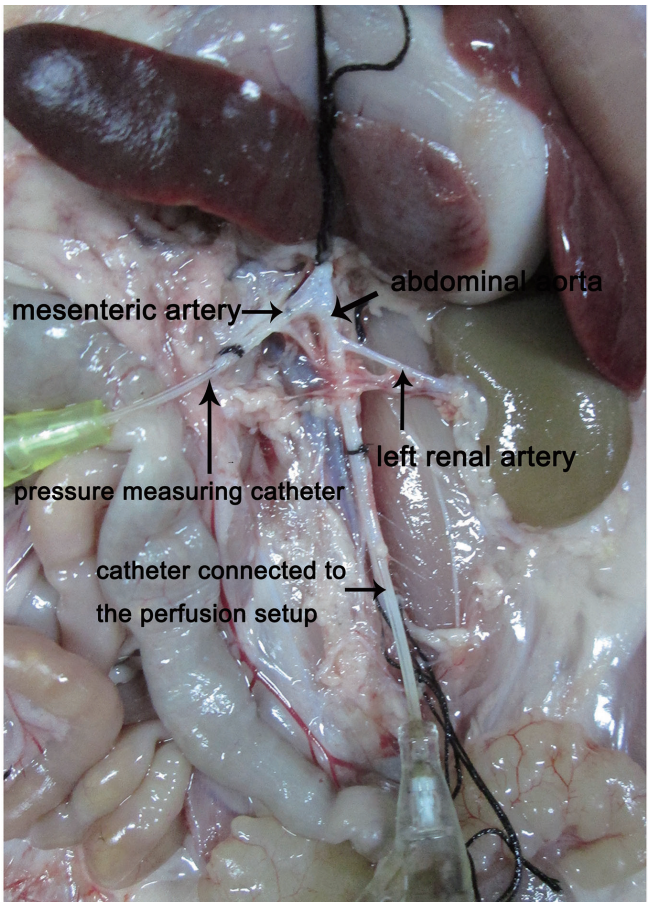

Fig. 1. The preparation process of the rats for minimal renal vascular resistance. The mesenteric artery was cannulated to allow measurement of aortic pressure close to the left renal artery (renal arterial inflow pressure). A catheter connected to the perfusion setup was inserted retrogradely through the abdominal aorta to a position distal to the left renal artery. The aorta was ligated just above the mesenteric artery to make a closed arterial circuit including the left kidney, and the left renal vein was cut.

microscope (DMI3000B, Leica, Germany) in a blind fashion to assess various characteristics of the arteries. Measurements of various parameters were performed by digital analysis. Both renal interlobular arteries (RILAs) and arcuate arteries (RAAs) were characterized by internal elastic laminas, which could be stained by EVG. RAAs (diameter 100-200 μm) were identified along the corticomedullary junction and were surrounded by tubules. RILAs (diameter 50-100 μm) were identified within the inner cortex (approximately 500 μm from the corticomedullary junction) and were surrounded by tubules. Arteries that were not sectioned transversely (long diameter/ short diameter>1.5) were excluded from the study.

After HE and EVG staining, 4 to 6 RAAs/RILAs were randomly selected from each animal and evaluated. Images of the arteries at 400× magnification were digitized and saved. According to the method of Alluru et al. (2001), the average morphological parameters of each sample, including the medial cross-sectional area percentage (CSA%, CSA%=medial cross-sectional area (CSA)/total cross-sectional area (CSA_{tot}), CSA=(CSA_{tot}-luminal cross-sectional area (CSA_{lum}))×(long internal diameter (ID_{long})/short internal diameter (ID_{short}))), medial thickness/external diameter (MT/ED, ED=2×(CSA_{tot}×ID_{short}/ID_{short}/π)1/2, MT=(ED-IDshort)/2) and medial thickness/internal diameter (MT/ID_{short}), were measured using Image-Pro Plus V 6.0 (IPP, Media Cybernetics Inc., USA) image analysis software.

Relative medial collagen area of RAAs and RILAs (Zou et al., 2015)

Arterial medial collagen fibres and vascular smooth muscle cells were red- or yellow-coloured after picric acid-Sirius red staining. The total collagen fibre area was determined based on the red area in the arterial tunica media. In each section, 4 to 6 RAAs/RILAs were randomly imaged to measure the average relative medial collagen area (equal to the medial collagen area/CSA) using IPP image analysis software.

Immunofluorescence staining (Lin et al., 2015)

The vascular smooth muscle cell (VSMC) layer was defined by the presence of α-smooth muscle actin (α-SMA), and α-SMA was detected by immunofluorescence staining. Briefly, slices were dewaxed and hydrated. After antigen retrieval at high pressure, the samples were blocked with goat serum. This was followed by dropwise addition of 100 μl of a mouse anti-α-SMA monoclonal antibody (1:2000 dilution, A2547, Sigma) and overnight incubation at 40°C. Phosphate-buffered saline was added instead of antibody in the blank control group. Then, 100 μl of tetramethyl rhodamine isothiocyanate fluorescence-labelled goat anti-mouse IgG secondary antibody (1:50 dilution, ZF-0313, Beijing Zhongshan Golden Bridge Biotechnology Inc.) was added, and the slices were incubated for 90 minutes in the dark at room temperature. After Tissue Autofluorescence Quencher (C1212, Beijing Applygen Technologies Inc.) was added and the slices were incubated in the dark at room temperature for 90 minutes, the slices were sealed using fluorescence decay-resistant glycerine (Beijing Applygen Technologies Inc.). Finally, images were acquired with an inverted fluorescence microscope (DMI3000B, Leica, Germany), and red fluorescence marked the locations of VSMCs.

Immunohistochemical staining (Zou et al., 2015)

As described above, paraffin slices were dewaxed, hydrated and subjected to antigen retrieval at high pressure. Then, the samples were incubated in 3% H_2O_2 for endogenous peroxidase removal and blocked with goat serum. Then, 100 μl of anti-AGE polyclonal antibody (1:100 dilution, 1158R, BosterBio), anti-RAGE polyclonal antibody (1:100 dilution, BA1789, BosterBio) or anti-PCNA monoclonal antibody (1:8000 dilution, PC10, Cell Signaling Technology) was added respectively to the slices, and the slices were incubated overnight at 4°C. Phosphate-buffered saline was added instead of antibody in the blank control group. This was followed by the successive addition of the auxiliary enhancer and secondary antibody (PV9001 was used for AGEs and RAGE; PV9002 was used for PCNA). Finally, DAB (AGE and RAGE stain) and AEC (PCNA stain) solutions were added to the slices dropwise, and the slices were counterstained with haematoxylin and mounted with neutral balsam and Clear-Mount, respectively. Positive staining for DAB was brown, while that for AEC was red. Thus, the positive areas for AGEs and RAGE were brown, while the positive areas for PCNA were red. Three slices were randomly selected for each sample, and 4 RAAs/RILAs from each slice were measured at 400× magnification using IPP software to calculate the average optical density (OD), the positive area (Area%) and the arterial medial cell proliferation index (PI). The OD and Area% were used as the measures of protein expression for AGEs and RAGE; the PI was equal to the number of medial PCNA-positive cells/the total number of medial cells and reflected the cell proliferation of the arterial media (Shapiro et al., 2008).

Measurement of plasma advanced glycation end products (AGEs)

At the end of the study, fasting blood samples were collected from the subjects before sacrifice. After centrifugation, the plasma was sub-packaged and stored at -80°C until use. Plasma AGEs were measured using a commercially available quantitative sandwich enzyme immunoassay (Quantikine, R&D systems, USA). Briefly, an anti-AGEs monoclonal antibody was precoated onto a microplate. Then, standards and samples, which were diluted to within the detection

range (1:1 dilution), were pipetted into the wells, and any AGEs present were bound by the immobilized antibody. After washing away any unbound substances, an enzyme-linked polyclonal antibody specific for AGEs was added to the wells. Following a wash to remove any unbound enzyme-linked antibody, a substrate solution was added to the wells, and the colour developed in proportion to the amount of AGEs bound in the initial step. The colour development was stopped, and the intensity of the colour (OD) was measured with a microplate reader (Bio-Rad 550, USA). According to the standard curve, the concentration of plasma AGEs in each sample was obtained (result×2, pg/ml). The intra-assay and inter-assay variation were 5.4% and 7.7%, respectively.

Statistical analysis

All data were presented as the mean ± standard deviation ($\bar{\chi}$±SD) and were analysed using SPSS 16.0 statistical software (SPSS Inc., Chicago, IL). The Levene test was used to test the homogeneity of variance. Two-way ANOVA and the SNK-q test were used to test the differences among different age groups in the same kind of rat when the assumption of homogeneity of variance was satisfied. Comparisons between two groups of different kinds of rats at the same age were conducted using independent sample t-tests. Differences with $p<0.05$ and $p<0.01$ were considered statistically significant and highly significant, respectively.

Results

Rat survival and blood pressure and weight changes

A total of 153 rats (out of 160 rats) survived throughout the experiments (total survival rate of 95.53%). As shown in Fig. 2, the systolic blood pressure (SBP), diastolic blood pressure (DBP) and mean arterial pressure (MAP) of SHRs were all increased by 12 weeks, peaked at 24 weeks (206.6±5.0 mmHg, 132.8±5.1 mmHg, 160.4±4.2 mmHg) and then plateaued, whereas the blood pressure of WKY rats remained at a normal level. The weights of both SHRs and WKY rats first increased, peaking at 48 weeks, and

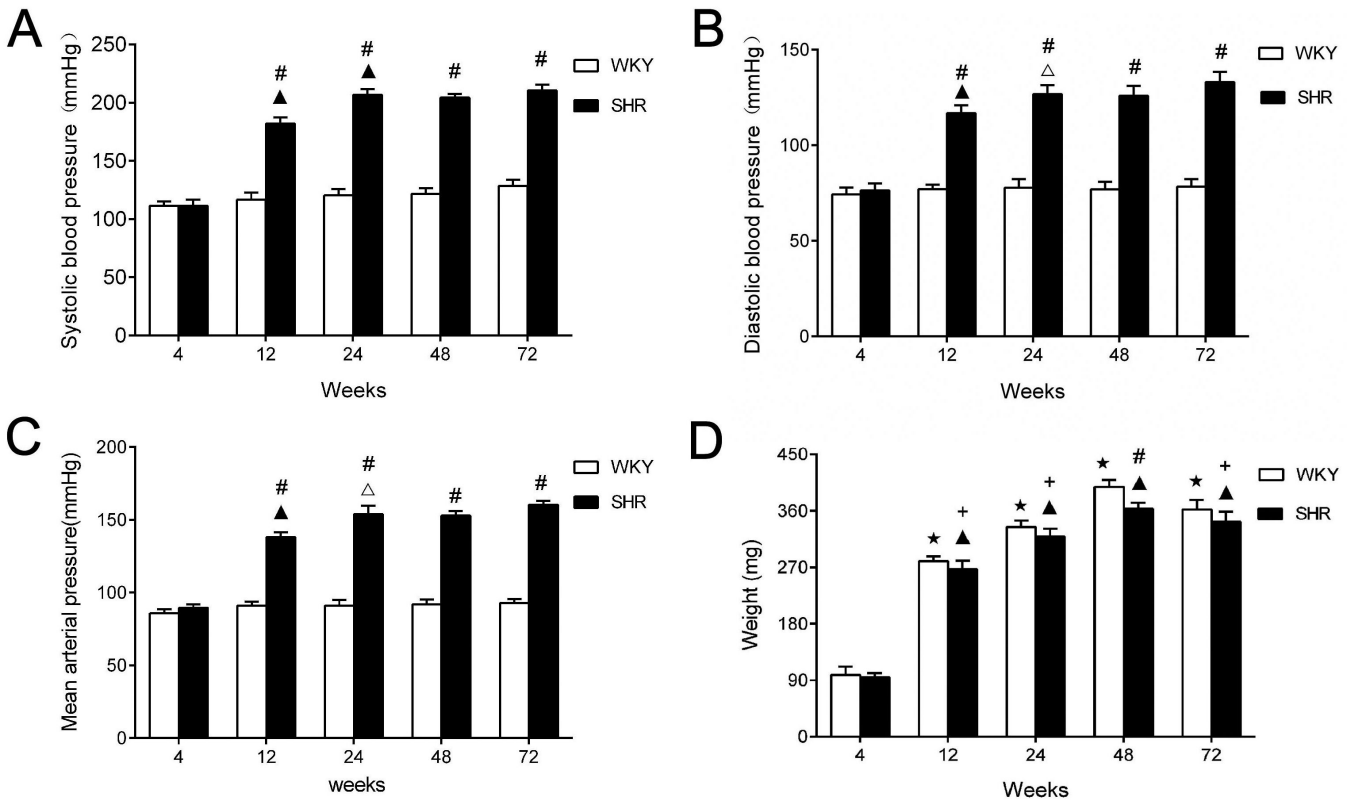

Fig. 2. Dynamic changes in blood pressure and weight in SHRs and WKY rats of different ages. Systolic blood pressure **(A)** Diastolic pressure **(B)** and mean arterial pressure **(C)** were increased with age in the SHRs, but not in WKY rats. **D.** The weights of both SHRs and WKY rats first increased, peaking at 48 weeks, and then decreased. All the data are presented as the $\bar{\chi}$±SD. ▲: $p<0.01$, compared to previous SHR group; △: $p<0.05$, compared to previous SHR group; ★: $p<0.01$, compared to previous WKY group; +: $p<0.05$, compared to the age-matched WKY group; #: $p<0.01$, compared to the age-matched WKY group.

then decreased. Except at 4 weeks, the weights of SHRs were lower than those of WKY rats ($p<0.05$), and the difference was most significant at 48 weeks ($p<0.01$).

The dynamic change in minimal renal vascular resistance with age

In the vasodilated kidneys of rats, the relationships between perfusion flow and arterial distending pressure showed a significant linear relationship with regression analysis in each individual experiment. Minimal renal vascular resistance (minRVR) was calculated as the slope of the trend line for the relationship between perfusion pressure and renal flow per unit (perfusion pressure/volume of renal flow per unit) (Huang et al., 2013). As shown in Fig. 3, in the SHR groups, minRVR gradually increased with age from 24 weeks ($p<0.05$) and was significantly higher than that in the WKY groups ($p<0.05$) at 12, 24, 48, and 72 weeks, but there was no difference at 4 weeks ($p>0.05$). In contrast, minRVR in WKY rats was increased by 72 weeks ($p<0.05$). From a functional perspective, it was demonstrated that IRSA stiffness occurred in both SHRs and WKY rats with age, but it occurred by 24 weeks, thus occurring much earlier, and was more severe in the SHR groups than in the WKY groups.

The morphological changes of IRSAs

As shown in Figs. 4-5 and Tables 1-2, the MT/ED, MT/IDshort, CSA%, medial cell proliferation index (PI) and relative medial collagen area of the RILA and RAA tunica media in SHRs had gradually increased by 24 weeks of age and peaked at 72 weeks, and the values of these indexes for SHRs at 24, 48 and 72 weeks were significantly higher than those for WKY rats of the same age ($p<0.05$). However, these indexes had increased by 72 weeks in the IRSAs of WKY rats. In addition, the relative medial collagen area of RILA was significantly higher at 12 weeks than at 4 weeks in SHRs ($p<0.05$)

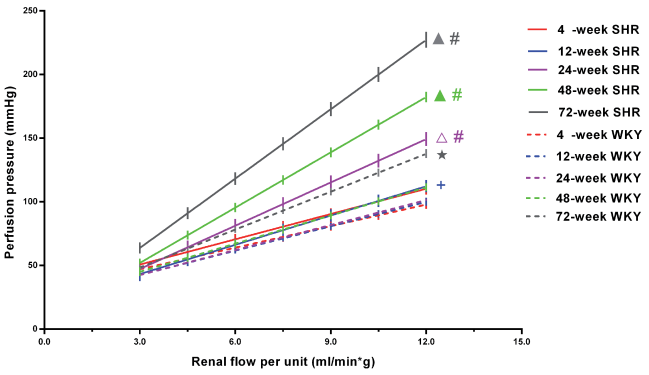

Fig. 3. Relationships between renal perfusate inflow per unit (x-axis) and arterial perfusion pressure (y-axis) in SHRs and WKY rats of different ages. All the data are presented as the $\bar{\chi}$±SD. ▲: $p<0.01$, compared to previous SHR group; △: $p<0.05$, compared to previous SHR group; ★: $p<0.01$, compared to previous WKY group; #: $p<0.01$, compared to the age-matched WKY group. +: $p<0.05$, compared to the age-matched WKY group.

Table 1. Dynamic changes of morphological indexes of RAAs in SHRs and WKY rats.

Weeks	Rat type	Number	Morphological indexes in RAAs CSA%(%)	MT/ED(%)	MT/ID_{short}(%)
4	WKY	8	19.15±2.46	10.38±2.28	11.29±1.93
	SHR	8	18.77±2.84	9.89±2.19	10.99±2.40
12	WKY	8	19.33±3.73	10.80±2.54	11.28±1.96
	SHR	7	21.08±3.11	12.09±2.68	13.22±2.65
24	WKY	7	19.29±3.24	10.98±2.43	11.21±1.98
	SHR	8	27.71±5.40△#	16.16±3.73△#	17.36±2.64△#
48	WKY	8	21.88±3.84	12.20±2.04	13.16±2.15
	SHR	6	35.66±4.59▲#	23.12±4.80△#	33.33±4.42▲#
72	WKY	7	27.76±3.74☆	17.23±3.44★	18.14±2.25★
	SHR	6	46.26±5.60▲#	32.69±4.12▲#	53.07±4.52▲#

In SHR groups, medial cross-sectional area percentage (CSA%), medial thickness/external diameter (MT/ED) and medial thickness/internal diameter (MT/ID_{short}) of the RAAs had gradually increased by 24 weeks. However, these indexes were increased only at 72 weeks in WKY rats. Number: the survival number of rats. All the data are presented as the $\bar{\chi}$±SD. ▲: $p<0.01$, compared to previous SHR group; △: $p<0.05$, compared to previous SHR group; ★: $p<0.01$, compared to previous WKY group; ☆: $p<0.05$, compared to previous WKY group; #: $p<0.01$, compared to the age-matched WKY group; +: $p<0.05$, compared to the age-matched WKY group.

Table 2. Dynamic changes of morphological indexes of RILAs in SHRs and WKY rats.

Weeks	Rat type	Number	Morphological indexes in RILAs CSA%(%)	MT/ED(%)	MT/ID_{short}(%)
4	WKY	8	20.22±3.14	11.91±1.83	12.63±2.16
	SHR	8	20.66±3.56	12.19±2.47	12.47±2.55
12	WKY	8	21.27±3.27	12.00±2.12	13.72±3.06
	SHR	7	24.77±3.50	14.62±3.37	15.44±2.91
24	WKY	7	22.43±3.63	12.91±2.45	13.70±2.22
	SHR	8	31.47±4.25△#	20.11±3.74△#	23.40±4.25△#
48	WKY	8	24.88±4.41	14.60±2.50	16.93±2.46
	SHR	6	41.29±4.50▲#	28.08±5.23△#	33.38±5.10▲#
72	WKY	7	31.20±4.56☆	18.50±3.96☆	23.75±5.05★
	SHR	6	54.69±4.03▲#	39.49±4.03▲#	61.68±5.37▲#

In SHR groups, medial cross-sectional area percentage (CSA%), medial thickness/external diameter (MT/ED) and medial thickness/internal diameter (MT/ID_{short}) of the RILAs had gradually increased by 24 weeks. However, these indexes were increased only at 72 weeks in WKY rats. Number: the survival number of rats. All the data are presented as the $\bar{\chi}$±SD. ▲: $p<0.01$, compared to previous SHR group; △: $p<0.05$, compared to previous SHR group; ★: $p<0.01$, compared to previous WKY group; ☆: $p<0.05$, compared to previous WKY group; #: $p<0.01$, compared to the age-matched WKY group.

and was also significantly higher than that of age-matched WKY rats ($p<0.05$). Therefore, ageing-related IRSAs remodelling and stiffness occurred in both SHRs and WKY rats with morphological changes including increased medial collagen and cell numbers, medial thickening and shrinkage of the inner diameter. In addition, the occurrence of IRSAs morphological remodelling and stiffness in SHRs was earlier than that in WKY rats, and the severity of remodelling and stiffness in SHRs was also greater than that in WKY rats.

Changes in plasma AGEs and dynamic AGEs and RAGE expression within the IRSAs tunica media

As shown in Figs. 6-8, in SHRs, the plasma levels of AGEs and the expression of AGEs within the tunica media of IRSAs were significantly increased from 48 weeks, and AGEs expression at 48 weeks and 72 weeks was significantly higher than that in age-matched WKY rats ($p<0.01$). The expression of RAGE in the tunica media of RAAs and RILAs was already increased by 24 weeks, and its expression at 24, 48 and 72 weeks was significantly higher in SHRs than in WKY rats ($p<0.05$). However, in WKY rats, except for the increased expression of AGEs in the RILA tunica media at 48 weeks, plasma AGEs and AGEs and RAGE expression in the IRSA media were increased only at 72 weeks. Additionally, the expression of RAGE in the RILA tunica media in SHRs was significantly higher at 12 weeks than at 4 weeks and was also significantly higher than that in WKY rats of the same age ($p<0.05$). These results demonstrated that ageing-related IRSA remodelling and stiffness in both rat strains were accompanied by increased expression of RAGE in the tunica media, whereas increases in IRSA medial AGEs expression and plasma AGEs levels occurred only at the late stage of arterial remodeling and stiffness.

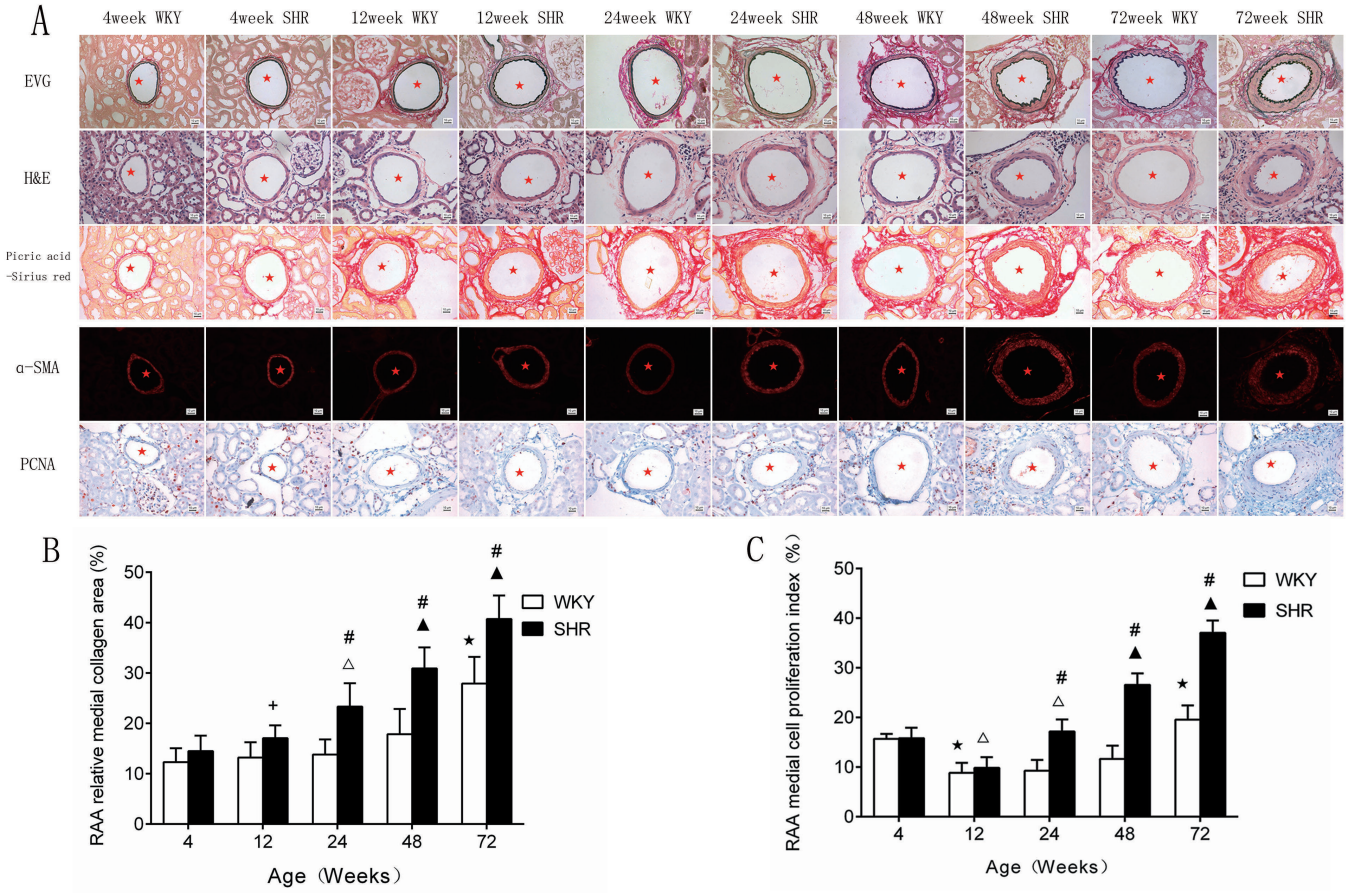

Fig. 4. Dynamic changes in the morphology of RAAs in SHRs and WKY rats. **A.** EVG, H&E, picric acid-Sirius red staining, α-SMA immunofluorescence staining (red) and PCNA immunohistochemical staining (red nuclei indicate cell proliferation) of the samples from each group. **B.** Dynamic changes in relative medial collagen area in RAAs of SHRs and WKY rats. **C.** Dynamic changes in the medial cell PI in RAAs of SHRs and WKY rats. All the data are presented as the $\bar{\chi}\pm SD$. ▲: $p<0.01$, compared to previous SHR group; △: $p<0.05$, compared to previous SHR group; ★: $p<0.01$, compared to previous WKY group; #: $p<0.01$: compared to the age-matched WKY group; +: $p<0.05$: compared to the age-matched WKY group. Scale bar: 10 μm.

Expression of RAGE within the tunica media occurred earlier in RILAs than in RAAs in SHRs, and the dynamic changes in RAGE expression in the IRSA tunica media were consistent with the morphological and functional changes.

Discussion

In this study, we used WKY rats and SHRs as models to study the occurrence and development of IRAS remodelling and stiffness during age progression. The study excluded a rapid ageing model based on accelerated metabolism and oxygen free radical generation and thus could truly reflect the changes in pathophysiological characteristics during natural ageing and hypertension. WKY rats and SHRs generally grew and experienced significant weight gain from 4 to 48 weeks, but the rats gradually became unresponsive, became shrivelled in appearance, developed dull hair that fell out easily and experienced significant weight loss from 48-72 weeks. Ageing and weight loss were more obvious in SHRs than in WKY rats (Fig. 2). Based on the related literature (Kieffer et al., 2000; Beuk et al., 2016; Létondor et al., 2016), the rats were divided into groups based on juvenile (4 w), adolescence (12 w), early adulthood (24 w), late adulthood (48 w) and old age (72 w) stages.

As small muscular arteries that govern blood redistribution in the organs, intrarenal small arteries (IRSAs), especially renal arcuate arteries (RAAs) and renal interlobular arteries (RILAs), are the important structures of renal nutrient supply and function implementation. It has been reported that the changes of blood pressure and the preglomerular vascular compliance with age in SHR led to glomerular hypertension, which resulted in glomerular injury and progressive loss of kidney function (Tolbert et al., 2000). The renal damage caused by ageing and hypertension is associated with

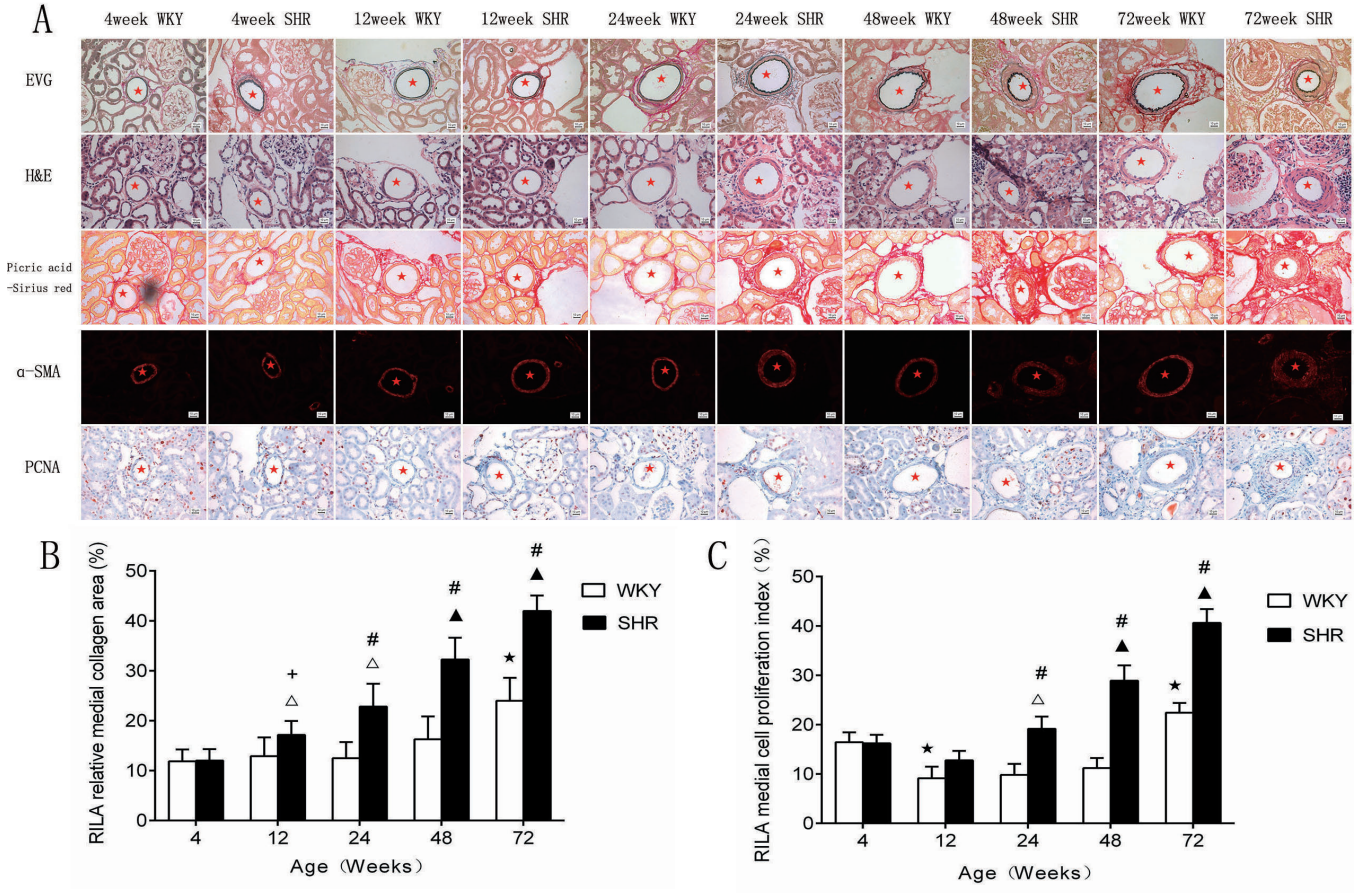

Fig. 5. Dynamic changes in the morphology of RILAs in SHRs and WKY rats. **A.** EVG, H&E, picric acid-Sirius red staining, α-SMA immunofluorescence staining and PCNA immunohistochemical staining of the samples from each group. **B.** Dynamic changes in the relative medial collagen area in RILAs of SHRs and WKY rats. **C.** Dynamic changes in the medial cell PI in RILAs of SHRs and WKY rats. All the data are presented as the $\bar{x}\pm SD$. ▲: $p<0.01$, compared to previous SHR group; △: $p<0.05$, compared to previous SHR group; ★: $p<0.01$, compared to previous WKY group; #: $p<0.01$: compared to the age-matched WKY group; +: $p<0.05$: compared to the age-matched WKY group. Scale bar: 10 μm.

IRSA pathological changes (Vavrinec et al., 2012). IRSA stiffness involves decreased vascular compliance caused by structural changes in the vascular wall. Its occurrence is not unique to ageing; stiffening can also occur due to high blood pressure, diabetes, renal insufficiency and smoking. In this study, we observed the minRVR and morphological indexes of RILAs and RAAs in WKY rats of different ages and found that the MT/ED, MT/ID_{short} and CSA% of RILAs and RAAs and the minRVR were significantly higher in 72-week-old WKY rats than in WKY rats of other ages (Fig. 3-5 and Tables 1-2). From the functional and morphological results, it was demonstrated that ageing induced IRSA stiffness in non-hypertensive rats that was characterized by concentric remodelling with medial thickening, consistent with what occurs in other small arteries (Moreau et al., 1998). To further study the effect of hypertension on renal arterial stiffness in aged rats, we compared the minRVR values and the morphology of IRSAs in SHRs and WKY rats at different ages. The results showed that the minRVR and the MT/ED, MT/IDshort, and CSA% of both IRSA types in SHRs were increased from 24 weeks, and the above indexes were higher in SHRs than in age-matched WKY rats (Figs. 3-5 and Tables 1-2, $p<0.05$). The results indicated that IRSA remodelling and stiffness occurred earlier and were more severe in ageing SHRs than in ageing WKY rats.

We found that there were no significant differences in the relative medial collagen area or cellular proliferation index (PI) of VSMCs between 4 and 48 weeks in RAAs and RILAs of WKY rats; in addition, the values of these parameters were significantly elevated only at 72 weeks compared to the other ages ($p<0.05$),

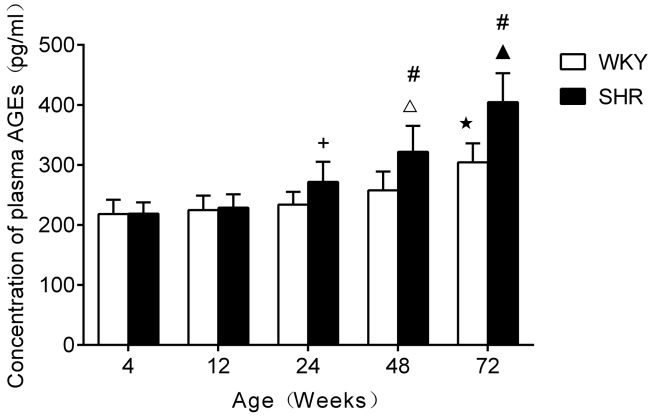

Fig. 6. Dynamic changes in the plasma levels of AGEs in SHRs and WKY rats of different ages.All the data are presented as the $\bar{\chi}\pm SD$. ▲: $p<0.01$, compared to previous SHR group; △: $p<0.05$, compared to previous SHR group; ★: $p<0.01$, compared to previous WKY group; #: $p<0.01$: compared to the age-matched WKY group; +: $p<0.05$: compared to the age-matched WKY group.

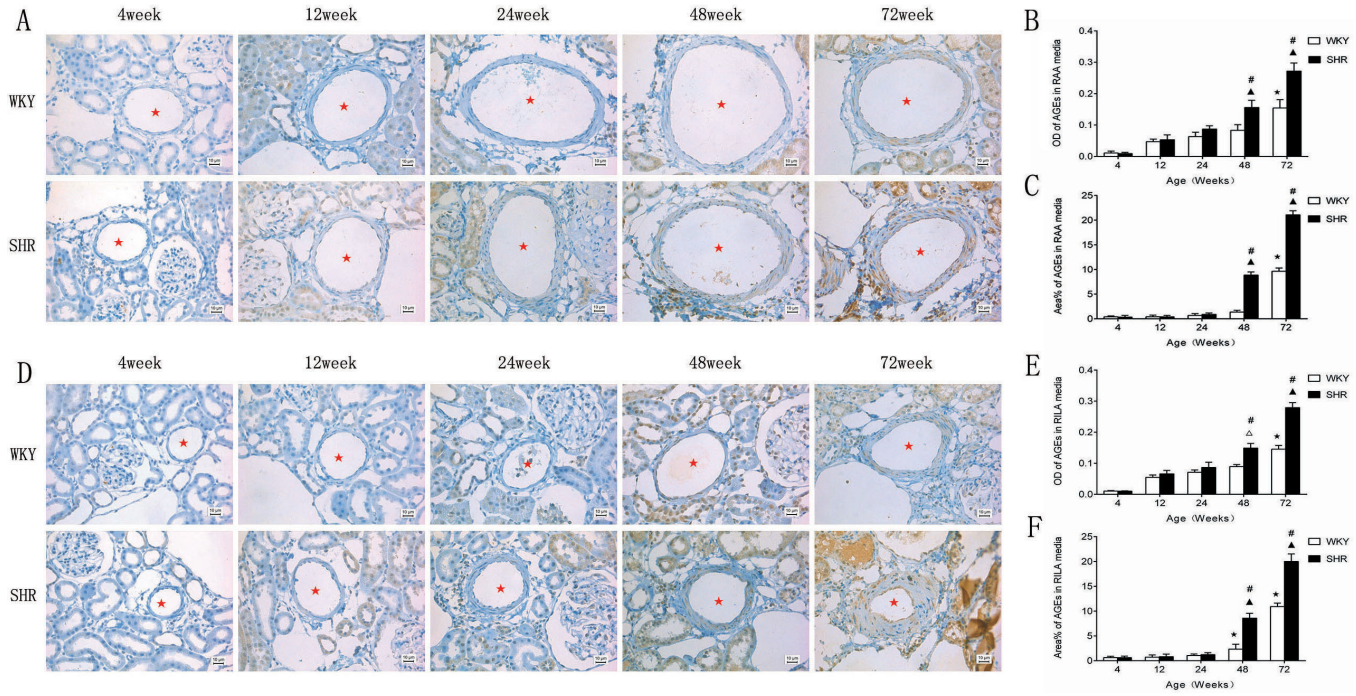

Fig. 7. Dynamic changes in AGE expression in IRSAs (RAAs and RILAs) of SHRs and WKY rats. A positive reaction in the cytoplasm appears as a brown stain. **A-C.** Dynamic changes in AGE expression in RAAs of SHRs and WKY rats. **D-F.** Dynamic changes in AGE expression in RILAs of SHRs and WKY rats. All the values are presented as the $\bar{\chi}\pm SD$. ▲: $p<0.01$, compared to previous SHR group; △: $p<0.05$, compared to previous SHR group; ★: $p<0.01$, compared to previous WKY group; #: $p<0.01$: compared to the age-matched WKY group. Scale bar: 10 μm.

consistent with the timing of vascular remodelling and arterial stiffening in WKY rats (Figs. 4-5). The results suggested that VSMCs and the extracellular matrix (ECM) were involved in the development of IRSA remodelling and stiffness. Previous studies have shown that the degrees of proliferation, stiffness and adhesion of VSMCs in elderly individuals are significantly higher than those in young individuals and are closely correlated with age-related arterial stiffness and related morphological changes (Qiu et al., 2010; Lei et al., 2012; Sehgel et al., 2015a,b). In addition, the increases in mechanical stress and reductions in elasticity caused by absolute and relative increases in collagen fibres and by changes in their direction of arrangement and ways of cross-linking are other important reasons for age-related arterial remodelling and stiffness (Robins, 2007). According to our study, ageing could also cause IRSA concentric remodelling with the characteristics of medial VSMC proliferation, collagen deposition and concentric medial thickening in rats. Moreover, we found that the above indexes of IRSAs in the SHR groups increased from 24 weeks and continuously increased with age. The values of these indexes were also higher than those in age-matched WKY rats ($p<0.05$, Figs. 4-5). The above results suggested that hypertension accelerated age-related IRSA remodelling and stiffness by accelerating VSMC abnormal proliferation and collagen deposition in the tunica media.This effect might be caused by increased arterial wall tone due to hypertension, chemical receptor mechanisms and other endocrine factors (Prado et al., 2006). Additionally, hypertension also could accelerate VSMC stiffness through SRF/myocardin signaling, leading to vascular stiffness (Zhou et al., 2017). It is worth mentioning that medial collagen in the RILAs of SHRs was increased at 12 weeks, whereas remodelling and stiffness-related morphological changes occurred until 24 weeks in the RAAs of SHRs (Figs. 4-5). This finding indicates that the acceleration and aggravation of age-related remodelling and stiffness mediated by hypertension occurred earlier in RILAs than in RAAs.

The mechanisms of ageing-induced renal small arterial remodelling and stiffness remain unclear. It has been shown recently that plasma AGEs can bind to the LDL receptor or to RAGE on VSMC membranes to promote proliferation, migration and differentiation of VSMCs through oxidative stress and proinflammatory action (Sima et al., 2010); conversely, plasma AGEs can directly deposit in vascular media in conjunction with medial AGEs derived from VSMCs (Hallam et al., 2010) and form AGEs-protein cross-links to cause accumulation of collagen protein and mediate the

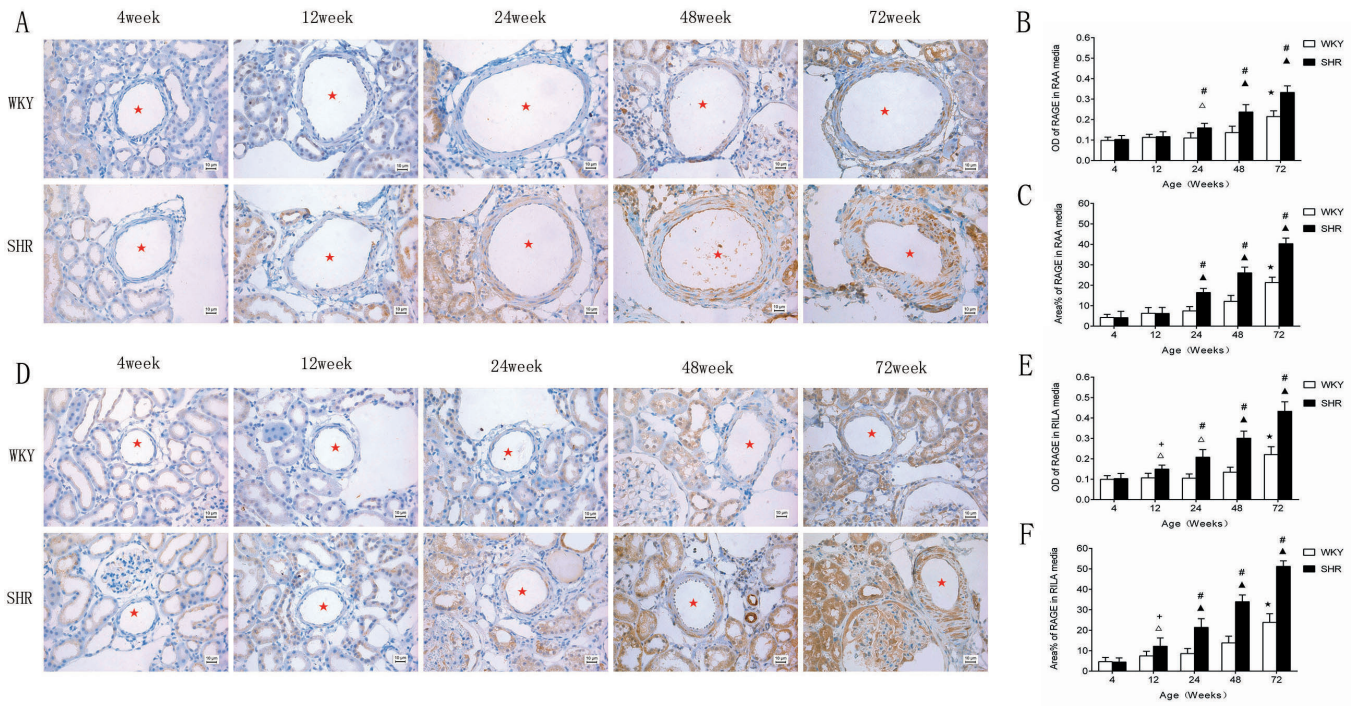

Fig. 8. Dynamic changes in RAGE expression in IRSAs (RAAs and RILAs) of SHRs and WKY rats. A positive reaction in the cytoplasm appears as a brown stain. **A-C.** Dynamic changes in RAGE expression in RAAs of SHRs and WKY rats. **D-F.** Dynamic changes in RAGE expression in RILAs of SHRs and WKY rats. All the values are presented as the $\bar{\chi}\pm SD$. ▲: $p<0.01$, compared to previous SHR group; △: $p<0.05$, compared to previous SHR group; ★: $p<0.01$, compared to previous WKY group; #: $p<0.01$: compared to the age-matched WKY group; +: $p<0.05$: compared to the age-matched WKY group. Scale bar: 10 μm.

dysfunction of VSMCs, ultimately resulting in arterial remodelling and stiffness (Lund et al., 2011; McRobert et al., 2012). In addition, AGEs in the tunica media can also induce abnormalities in VSMC proliferation and apoptosis and increase collagen synthesis and vascular tone through intracellular signalling pathways by interacting with RAGE, ultimately leading to increases in vascular wall mechanical strength and compliance reduction (Sun et al., 2016; Li et al., 2017). In our study, we found that the plasma concentration of AGEs and the expression of AGEs and RAGE in the IRSA tunica media in 72-week-old WKY rats (elderly rats) were significantly increased (Fig. 6-8), and these increases were accompanied by increases in medial PI and medial collagen deposition, consistent with the process of IRSA stiffening and remodelling. The results suggested that plasma AGEs and RAGE and AGEs expression within the tunica media of IRSAs were associated with age-related remodelling and stiffness development. Notably, there was no altered expression of RAGE or remodelling and stiffness when the expression of AGEs in the RILA tunica media was upregulated in 48-week-old WKY rats (Figs. 3, 5, 7, 8). These results suggested that AGEs deposited in the media probably did not interact with RAGE in VSMC membranes but rather directly cross-linked with collagen and mediated IRSA remodelling and stiffness. This hypothesis needs to be further studied in the future.

We also found that the medial expression of RAGE in the RILAs and RAAs of SHRs was markedly upregulated after 12 weeks and 24 weeks, respectively. Furthermore, RAGE expression in the IRSA tunica media in SHRs at 24, 48 and 72 weeks was significantly higher than that in age-matched WKY rats ($p<0.05$, Fig. 8), consistent with the timing of IRSA remodelling and stiffening. However, the levels of AGEs in both plasma and the IRSA tunica media started increasing from 48 weeks in SHRs (Fig. 6-7), which demonstrated that hypertension did not simply accelerate IRSA remodelling and stiffness through activating the AGEs-RAGE pathway. As discovered by Meloche et al. (2013) and Chang et al. (2011) in studies on pulmonary hypertension patients and hypertensive rat models with the aortic sinus and arch nerve removed, soluble RAGE (sRAGE) can significantly inhibit the proliferation of VSMCs and improve compliance. Compared to AGEs, RAGE may play a more important role in hypertension-induced acceleration and aggravation of ageing-related IRSA remodelling and stiffness. As a multi-ligand receptor, RAGE has been shown to directly cause arterial stiffness by binding a variety of other ligands with β-sheet structures (Li et al., 2012; Liu et al., 2013; Chaabane et al., 2015) or by causing haemodynamic abnormalities and hormonal stimulation under hypertensive conditions (Belmadani et al., 2008; Hayakawa et al., 2012). In addition, RAGE-mediated downstream pathways can engage in cross-talk. For example, activated ERK1/2 can in turn activate chymotrypsin, the renin-angiotensin system and oxidative stress pathways, which further increases the formation of AGEs and RAGE. This vicious cycle aggravates arterial remodelling and stiffness. The aggravation of arterial remodelling and stiffness could further stimulate increases in the above factors and in RAGE formation (Koka et al., 2006). Therefore, RAGE in the IRSA tunica media might also participate in the process of ageing-related IRSA remodelling and stiffening through other mechanisms aside from AGEs binding, which also explains the different changes in RAGE and AGEs in the IRSA tunica media during ageing with hypertension. It is worth mentioning that in SHRs, the upregulation of medial RAGE expression in RILAs began at 12 weeks (Fig. 8), which was consistent with RILA remodelling (the increase in the relative medial collagen area), while it began at 24 weeks in RAAs. This result might have been related to activation of RAGE resulting from greater blood flow-induced mechanical stretch in RILAs than in RAAs that was caused by a greater proximal pressure difference in RILAs than in RAAs (Heyeraas and Aukland, 1987).

In the present study, we found that hypertension could accelerate and aggravate the occurrence and development of arterial remodelling and stiffness of IRSAs in aged rats. This effect was accompanied by upregulation of medial RAGE expression on the vessel wall that started at 24 weeks, while plasma AGEs levels and AGEs expression on the vessel wall began to increase at 48 weeks. The hypertension-mediated acceleration and aggravation of IRSA remodelling and stiffness might have been related to the upregulation of RAGE expression in hypertensive rats during ageing, while the subsequent increases in AGEs levels in the circulation and the vascular wall further aggravated remodelling and stiffening. Furthermore, hypertension-mediated acceleration and aggravation of remodelling and stiffness occurred earlier in renal interlobular arteries than in arcuate arteries.

Acknowledgements. The study Sponsored by National Natural Science Foundation of China (No. 81170143, 81570448), National Key Clinical Specialty Discipline Construction Programs (2013544) and Fujian Province's Key Clinical Specialty Discipline Construction Programs (2012149).

References

Belmadani S., Zerfaoui M., Boulares H.A., Palen D.I. and Matrougui K. (2008). Microvessel vascular smooth muscle cells contribute to collagen type I deposition through ERK1/2 MAP kinase, alphavbeta3-integrin, and TGF-beta1 in response to ANG II and high glucose. Am. J. Physiol. Heart Circ. Physiol. 295, 69-76.

Beuk J., Beninger R. and Paré M. (2016). Lifespan changes in the countermanding performance of young and middle aged adult rats. Front. Aging Neurosci. 8, 190.

Bruno R.M., Duranti E., Ippolito C., Segnani C., Bernardini N., Di Candio G., Chiarugi M., Taddei S. and Virdis A. (2017). Different impact of essential hypertension on structural and functional age-related

vascular changes. Hypertension 69, 71-78.

Chaabane C., Heizmann C.W. and Bochaton-Piallat M.L. (2015). Extracellular S100A4 induces smooth muscle cell phenotypic transition mediated by RAGE. Biochim. Biophys. Acta 1853, 2144-2157.

Chang T., Wang R., Olson D.J., Mousseau D.D., Ross A.R. and Wu L. (2011). Modification of Akt1 by methylglyoxal promotes the proliferation of vascular smooth muscle cells. FASEB J. 25, 1746-1757.

Chilton L., Smirnov S.V., Loutzenhiser K., Wang X. and Loutzenhiser R. (2011). Segment-specific differences in the inward rectifier K+ current along the renal interlobular artery. Cardiovasc. Res. 92, 169-177.

Denic A., Glassock R.J. and Rule A.D. (2016). Structural and functional changes with the aging kidney. Adv. Chronic Kidney Dis. 23,19-28.

Franchi F., Zhu X.Y., Witt T.A., Lerman L.O. and Rodriguez-Porcel M. (2016). Intravascular delivery of biologics to the rat kidney. J. Vis. Exp. 1. 54418.

Hallam K.M., Li Q., Ananthakrishnan R., Kalea A., Zou Y.S., Vedantham S., Schmidt A.M., Yan S.F. and Ramasamy R. (2010). Aldose reductase and AGE-RAGE pathways: central roles in the pathogenesis of vascular dysfunction in aging rats. Aging Cell 9, 776-784.

Hayakawa E., Yoshimoto T., Sekizawa N., Sugiyama T. and Hirata Y. (2012). Overexpression of receptor for advanced glycation end products induces monocyte chemoattractant protein-1 expression in rat vascular smooth muscle cell line. J. Atheroscler. Thromb. 19, 13-22.

Heyeraas K.J. and Aukland K. (1987). Interlobular arterial resistance: influence of renal arterial pressure and angiotensin II. Kidney Int. 31, 1291-1298.

Huang Q.F., Sheng C.S., Liu M., Li F.H., Li Y. and Wang J.G. (2013). Arterial stiffness and wave reflections in relation to plasma advanced glycation end products in a Chinese population. Am. J. Hypertens. 26, 754-761.

Janić M., Lunder M. and Sabovič M. (2014). Arterial stiffness and cardiovascular therapy. Biomed. Res. Int. 2014, 621437.

Kieffer P., Robert A., Capdeville-Atkinson C., Atkinson J. and Lartaud-Idjouadiene I. (2000). Age-related arterial calcification in rats. Life Sci. 66, 2371-2381.

Koka V., Wang W., Huang X.R., Kim-Mitsuyama S., Truong L.D. and Lan H.Y. (2006). Advanced glycation end products activate a chymase-dependent angiotensinII-generating pathway in diabetic complications. Circulation 113, 1353-1360.

Lei Y., Tao L.L. and Wang G.L. (2012). Effect of extracts from Panax ginseng, Panax notoginseng, and ligusticum chuanxiong on vascular smooth muscle cells of aging and hypertension rats. Zhongguo Zhong Xi Yi Jie He Za Zhi 32, 1374-1379

Létondor A., Buaud B., Vaysse C., Richard E., Layé S., Pallet V. and Alfos S. (2016). EPA/DHA and vitamin a supplementation Improves satial memory and alleviates the age-related decrease in hippocampal RXRγ and kinase expression in rats. Front. Aging Neurosic. 8, 103.

Li Y., Liu S., Zhang Z., Xu Q., Xie F., Wang J., Ping S., Li C., Wang Z., Zhang M., Huang J., Chen D., Hu L. and Li C. (2012). RAGE mediates accelerated diabetic vein graft atherosclerosis induced by combined mechanical stress and AGEs via synergistic ERK activation. PLoS One 7, e35016.

Li C., Chang Y., Li Y., Chen S., Chen Y., Ye N., Dai D. and Sun Y. (2017). Advanced glycation end products promote the proliferation and migration of primary rat vascular smooth muscle cells via the upregulation of BAG3. Int. J. Mol. Med. 39, 1242-1254.

Lin X.H., Hong H.S., Zou G.R. and Chen L.L. (2015). Upregulation of TRPC1/6 may be involved in arterial remodeling in rat. J. Surg. Res. 195, 334-343.

Liu M., Yu Y., Jiang H., Zhang L., Zhang P.P., Yu P., Jia J.G., Chen R.Z., Zou Y.Z. and Ge J.B. (2013). Simvastatin suppresses vascular inflammation and atherosclerosis in ApoE(-/-) mice by downregulating the HMGB1-RAGE axis. Acta. Phamacol. Sin. 34, 830-836.

Lund T., Svindland A., Pepaj M., Jensen A.B., Berg J.P., Kilhovd B. and Hanssen K.F. (2011). Fibrin(ogen) may be an important target for methylglyoxal-derived AGE modification in elastic arteries of humans. Diab. Vasc. Dis. Res. 8, 284-294.

Ma M., Guo X., Chang Y., Li C., Meng X., Li S., Du Z.X., Wang H.Q. and Sun Y. (2015). Advanced glycation end products promote proliferation and suppress autophagy via reduction of Cathepsin D in rat vascular smooth muscle cells. Mol. Cell. Biochem. 403, 73-83.

McRobert E.A., Young A.N. and Bach L.A. (2012). Advanced glycation end-products induce calpain-mediated degradation of ezrin. FEBS J. 279, 3240-3250.

Meloche J., Courchesne A., Barrier M., Carter S., Bisserier M., Paulin R., Lauzon-Joset J.F., Breuils-Bonnet S., Tremblay É., Biardel S., Racine C., Courture C., Bonnet P., Majka S.M., Deshaies Y., Picard F., Provencher S. and Bonnet S. (2013). Critical role for the advanced glycation end-products receptor in pulmonary arterial hypertension etiology. J. Am. Heart Assoc. 2, e005157.

Moreau P., d'Uscio L.V. and Lüscher T.F. (1998). Structure and reactivity of small arteries in aging. Cardiovasc. Res. 37, 247-253.

Prado C.M., Ramos S.G., Alves-Filho J.C., Elias J. Jr, Cunha F.Q. and Rossi M.A. (2006). Turbulent flow/low wall shear stress and stretch differentially affect aorta remodeling in rats. J. Hypertens. 24, 503-515.

Qiu H., Zhu Y., Sun Z., Trzeciakowski J.P., Gansner M., Depre C., Resuello R.R., Natividad F.F., Hunter W.C., Genin G.M., Elson E.L., Vatner D.E., Meininger G.A. and Vatner S.F. (2010). Short communication: vascular smooth muscle cell stiffness as a mechanism for increased aortic stiffness with aging. Circ. Res. 107, 615-619

Reddi A.S., Nimmagadda V.R. and Arora R. (2001). Effect of antihypertensive therapy on renal artery structure in type 2 diabetic rats. Hypertension 37, 1273-1278.

Robins S.P. (2007). Biochemistry and functional significance of collagen cross-linking. Biochem. Soc. Trans. 35, 849-852

Sehgel N.L., Sun Z., Hong Z., Hunter W.C., Hill M.A., Vatner D.E., Vatner S.F., Meininger GA. (2015a). Augmented vascular smooth muscle cell stiffness and adhesion when hypertension is superimposed on aging. Hypertension 65, 370-377.

Sehgel N.L., Vatner S.F. and Meininger G.A. (2015b). "Smooth Muscle Cell Stiffness Syndrome"—Revisiting the Structural Basis of Arterial Stiffness. Front. Physiol. 6, 335.

Shapiro B.P., Owan T.E., Mohammed S.F., Meyer D.M., Mills L.D., Schalkwijk C.G. and Redfield M.M. (2008). Advanced glycation end products accumulate in vascular smooth muscle and modify vascular but not ventricular properties in elderly hypertensive canines. Circulation 118, 1002-1010.

Shi X., Bai Y., Ke Y., Chen R., Lin X., Chen L. and Hong H. (2018). Ageing-related aorta remodelling and calcification occur earlier and

progress more severely in rats with spontaneous hypertension. Histol. Histopathol. 33, 727-736.

Sima A.V., Botez G.M., Stancu C.S., Manea A., Raicu M. and Simionescu M. (2010). Effect of irreversibly glycated LDL in human vascular smooth muscle cells: lipid loading, oxidative and inflammatory stress. J. Cell. Mol. Med. 14, 2790-2802.

Singh R., Barden A., Mori T. and Beilin L. (2001). Advanced glycation end-products: A review. Diabetologia 44, 129-146.

Skov K., Mulvany M.J. and Korsgaard N. (1992). Morphology of renal afferent arterioles in spontaneously hypertensive rats. Hypertension 20, 821-827.

Song H.F., Chen J.F., Sun N.L. and Li H.W. (2011). Effects of angiotensin II receptor antagonist olmesartan on renal hemodynamic variables and vascular structural properties in streptozotocin-induced diabetic rats. Chin. Med. J. 124, 562-567.

Sun Y., Kang L., Li J., Liu H., Wang Y., Wang C. and Zou Y. (2016). Advanced glycation end products impair the functions of saphenous vein but not thoracic artery smooth muscle cells through RAGE/MAPK signalling pathway in diabetes. J. Cell. Mol. Med. 20, 1945-1955.

Tolbert E.M., Weisstuch J., Feiner H.D. and Dworkin L.D. (2000). Onset of glomerular hypertension with aging precedes injury in the spontaneously hypertensive rat. Am. J. Physiol. Renal Physiol. 278, 839-846.

Vavrinec P., Henning R.H., Goris M., Vavrincova-Yaghi D., Buikema H. and van Dokkum R.P. (2012). Vascular smooth muscle function of renal glomerular and interlobar arteries predicts renal damage in rats. Am. J. Physiol. Renal Physiol. 303, 1187-1195.

Wu F., Feng J.Z., Qiu Y.H., Yu F.B., Zhang J.Z., Zhou W., Yu F., Wang G.K., An L.N., Ni F.H., Wu H., Zhao X.X., Qin Y.W. and Luo H.D. (2013). Activation of receptor for advanced glycation end products contributes to aortic remodeling and endothelial dysfunction in sinoaortic denervated rats. Atherosclerosis 229, 287-294.

Zhou N., Lee J.J., Stoll S., Ma B., Costa K.D. and Qiu H. (2017). Rho kinase regulates aortic vascular smooth muscle cell stiffness via actin/SRF/myocardin in hypertension. Cell. Physiol. Biochem. 44, 701-715.

Zou G., Hong H., Lin X., Shi X., Wu Y. and Chen L. (2015). TRPC1, CaN and NFATC3 signaling pathway in the pathogenesis and progression of left entricular hypertrophy in spontaneously hypertensive rats. Clin. Exp. Hypertens. 37, 223-234.

Accepted June 27, 2019